J Radioanal Nucl Chem (2013) 295:369–377
DOI 10.1007/s10967-012-1854-3

Adsorption kinetics and equilibrium modeling of cesium on copper ferrocyanide

Fei Han · Guang-Hui Zhang · Ping Gu

Received: 20 March 2012 / Published online: 25 May 2012

Abstract The copper ferrocyanide (CuFC) prepared in this study was characterized using X-ray diffraction and scanning election microscopy. The distribution of particle sizes of the CuFC suspension was determined. The adsorption kinetics data were evaluated for an intraparticle diffusion model, a pseudo-first order model and a pseudo-second order model at temperatures of 288, 298 and 308 K, respectively. It was found that the adsorption process of Cs^+ on CuFC was best described by a pseudo-second order kinetic model, with a correlation coefficient (R^2) equal to 1.000, and the adsorption rate constant increased with increasing temperature. This result indicated that chemisorptions took place during the adsorption process. The adsorption equilibrium data fit well to the Langmuir, Freundlich and Dubinin-Radushkevich (D-R) isotherm models. The mean adsorption energy (E) between 11 and 13 kJ/mol at different temperatures indicated that ion exchange was the main mechanism during the adsorption process. Thermodynamic parameters were also evaluated during the adsorption. The values of the standard Gibbs free energy change (ΔG^o) and standard enthalpy change (ΔH^o) suggested that the adsorption was a spontaneous and endothermic process. The distribution coefficient (K_d) was more than 2.94×10^6 mL/g when the pH of solution was between 2.6 and 10.9, and the initial Cs^+ concentration was 100 μg/L. The existence of K^+ and Na^+ did not affect the adsorption of Cs^+ on CuFC when the concentration of K^+ and Na^+ in the solution was below 20 and 1,000 mg/L, respectively.

F. Han · G.-H. Zhang · P. Gu (✉)
School of Environmental Science and Engineering, Tianjin University, Tianjin 300072, China
e-mail: guping@tju.edu.cn

Keywords Cesium · Copper ferrocyanide · Adsorption · Kinetics · Isotherms

Introduction

Nuclear facilities and accidents produce a number of liquid wastes. These liquid wastes require treatment to remove radioactive contaminants before discharge. Cesium is one of the most abundant radionuclides found in nuclear fission products that are routinely or accidentally released, the latest example of the latter being that of the Fukushima Daiichi Nuclear Power Plant accident [1]. Radiocesium has a long half-life (^{137}Cs $T_{1/2}$ ~30.1 years, ^{135}Cs $T_{1/2}$ ~2.1×10^6 years) and is considered a hazardous element to the environment and human health [2, 3]. There are several methods for removing cesium from liquid waste. Precipitation of cesium with tetraphenylborate (TPB) was developed for large-scale cesium removal at the Savannah River Site in the early 1980s [4]. Although the process resulted in decontamination, the decomposition of TPB, catalyzed by noble metal fission products, led to the suspension of work on the process early in 1998 [5]. Most of the extractants used in the process of solvent extraction have been undesirable organics, which have a complex composition and are highly toxic. Additionally, the extractants are often difficult to prepare and commercially unavailable [6, 7]. Crystalline silicotitanate (CST) is excellent for the adsorption of cesium, with a distribution coefficient (K_d) of up to 10^5–10^6 mL/g [8, 9]; however, a major drawback of using CST is that the time to reach adsorption equilibrium can be as long as 10–12 days [9]. Natural or synthetic zeolite, inorganic phosphate and composite ion exchangers can selectively adsorb cesium from solution

with a K_d of 10^2–10^4 mL/g [10–12]. However, their adsorption capacity is low and is remarkably affected by the acidity and salinity of the solution.

In recent decades, there have been many reports of transition metal ferrocyanides for removing cesium from solution [13–24]. Transition metal ferrocyanides exhibit good adsorption properties for cesium because they have a high affinity for cesium over a wide pH range [24]. Zhang et al. [22] used potassium zinc hexacyanoferrate combined with microfiltration to remove cesium from liquid waste. Vrtoch et al. [23] prepared potassium nickel hexacyanoferrate-loaded biosorbent to remove cesium in the solution, and they discussed the kinetics and the adsorption equilibrium of the biosorbent. Lee et al. [20, 21] performed a series of studies on the adsorption mechanism and kinetics of potassium copper ferrocyanide (KCuFC) and compared the cesium adsorption characteristic of the KCuFC with that of copper ferrocyanide (CuFC) and potassium cobalt ferrocyanide. Loos-Neskovic et al. [16, 19] discussed the crystal structure of KCuFC and the adsorption mechanism of cesium. Sinha et al. [17] studied freshly precipitated CuFC for the removal of cesium from radioactive liquid waste. Ayrault et al. [19] believed that CuFC was one of the most promising compounds for the recovery of cesium from nuclear liquid wastes. However, the kinetics model and the adsorption isotherms of cesium adsorption to CuFC have seldom been reported.

In this study, CuFC was prepared as an adsorbent for Cs^+ in solution. The kinetics and adsorption isotherm models of Cs^+ adsorption onto CuFC were determined. The type of adsorption reaction was determined via thermodynamic parameters obtained at different temperatures. The influence of pH and the co-existence of K^+ or Na^+ in the solution on the adsorption of Cs^+ on CuFC were studied.

Experimental methods

Chemical reagents and preparation of the cesium solution

High-purity cesium nitrate reagent was purchased from Tianjin Kermel Chemical Reagents CO., LTD., China. Sodium ferrocyanide, copper nitrate, sodium chloride, potassium chloride, sodium hydroxide, hydrochloric acid and hydrogen nitrate were analytical reagents and were purchased from Tianjin Guangfu Fine Chemical Research Institute, China. The cesium-containing solution used in this study was prepared by dissolving cesium nitrate into distilled water. The Cs^+ concentration was 100 μg/L, and the pH of the solution was approximately 6.5.

Preparation of adsorbent

Solutions of 0.125 mol/L sodium ferrocyanide in a volume of 0.130 L and 0.375 mol/L copper nitrate in a volume of 0.124 L were mixed in a beaker containing 2 L ultrapure water by slow, simultaneous addition at a speed of approximately 0.1 mL/min, with gentle mechanical stirring. The temperature of the solution was maintained at 55 °C using a water bath. The precipitates were washed with ultrapure water 8 times using a total washing volume of 2 L [18]. After that, the CuFC suspension was ready for use.

Adsorption experiment

The adsorption experiments were conducted with a timed, adjustable speed mixer (model DBJ-621, China) at a speed of 150 r/min. After stirring for a certain amount of time, all of the solution was filtered, and the Cs^+ concentration was measured. The experiments were performed twice, and the results were reported as average values.

Adsorption kinetics

The CuFC suspension (magnetic stirring was used to keep the CuFC suspended and uniform) had a dose of 80 mg/L and was added into 200 mL of the cesium containing solution, and the mixed liquor was stirred at different times (5–120 min). The temperature of the solution was maintained at 288, 298 and 308 K, respectively, with a water bath. The adsorption capacity q_t (μg/g) of the CuFC at time t was determined by Eq. (1):

$$q_t = \frac{(C_0 - C_t)V}{m} \quad (1)$$

where C_0 and C_t are the Cs^+ concentration in the solution at the initial time and at time t, respectively (μg/L); V is the volume of the solution (L); and m is the mass of the adsorbent (g).

Adsorption equilibrium

Different doses of CuFC (2–80 mg/L) were mixed with 200 mL of the cesium containing solution at temperatures of 288, 298 and 308 K. The mixed liquor was stirred for 90 min. The equilibrium adsorption capacity q_e (μg/g) was determined by Eq. (2):

$$q_e = \frac{(C_0 - C_e)V}{m} \quad (2)$$

where C_e is the equilibrium concentration of Cs^+ in the solution (μg/L).

Effect of pH

The experiments to determine the effect of pH on the adsorption of Cs^+ were conducted by adding 80 mg/L CuFC into 200 mL of the cesium containing solution at different pH (2–13), and the mixture was stirred for 90 min at 298 K. The pH of the initial solution was adjusted with a suitable quantity of NaOH or HCl.

Effect of K^+ and Na^+

To discuss the effect of the existence of K^+ or Na^+ in the solution on the adsorption of Cs^+, different masses of KCl or NaCl were added into 200 mL of the cesium containing solution to adjust the concentration of K^+ and Na^+ in the solution to between 2.5 and 400 mg/L and 10–2,000 mg/L, respectively. Then, 80 mg/L of CuFC was added to the solution, and the mixture was stirred for 90 min at 298 K.

Analysis methods

An X-ray spectrometer (Model ISIS300, Oxford, England) was used to analyze the chemical composition of the CuFC. The phase was identified with a JCPDS-ICDD database. The particle morphology and the distribution of particle sizes of the adsorbent were analyzed with a scanning electron microscope (SEM) (Model XL-30, Phillips, Netherlands) and a laser size analyzer (Model Mastersizer 2000, Malvern, England), respectively.

The cesium was analyzed with an X7 Series inductively coupled plasma mass spectrophotometer (ICP-MS) (Thermo Electron Corporation, USA), and all of the samples were filtered with flat microfiltration membranes (0.22 μm, polyvinylidene fluoride, China) before analysis. The potassium and sodium concentrations were measured on a Zeeman atomic adsorption spectrometer (Model 180-80, Hitachi, Japan). The pH values were measured on a precise pH meter (Model PHS-3C, Sartorius, Germany).

The adsorption efficiency of Cs^+ on CuFC was evaluated by Eq. (3):

$$K_d = \frac{(C_0 - C_e)\,V}{C_e\,m} \times 1000 \quad (3)$$

where K_d is the distribution coefficient (mL/g) and represents the ratio of the Cs^+ concentration in the solid phase of the CuFC to the residual Cs^+ concentration in the solution.

Results and discussion

Characterizations of the adsorbent

X-ray crystallographic analyses

The possible products prepared with solutions of $Na_4Fe(CN)_6$ and $Cu(NO_3)_2$ are $Cu_2Fe(CN)_6{\cdot}xH_2O$, Na_2Cu-$Fe(CN)_6{\cdot}xH_2O$ or a mixture of both. However, pure $Cu_2Fe(CN)_6{\cdot}xH_2O$ could be acquired through careful washing procedures [17, 19]. The product prepared in this study was $Cu_2Fe(CN)_6{\cdot}7H_2O$, as determined by the X-ray diffraction (XRD) analysis (Fig. 1) and compared with JCPDS-ICDD 1.0244. The yield was approximately 100 %, and similar results were reported by Ayrault et al. [18].

Morphology

The SEM image of prepared CuFC is shown in Fig. 2. The CuFC particles had well-defined geometric shapes with a single particle dimension of approximately 30 nm. The agglomeration of particles is shown in Fig. 2, and this result was similar to another study [16].

The particle size distribution of the adsorbent suspended solution

The particle size distribution of the CuFC suspension was determined from the CuFC suspension that was used as the adsorbent in this study. The result is shown in Fig. 3.

The particle size followed a normal distribution. The minimum and maximum particle sizes were 0.55 and 45 μm, respectively. The volume fraction was 50 %, with particle sizes between 0.55 and 11.235 μm. The pore size

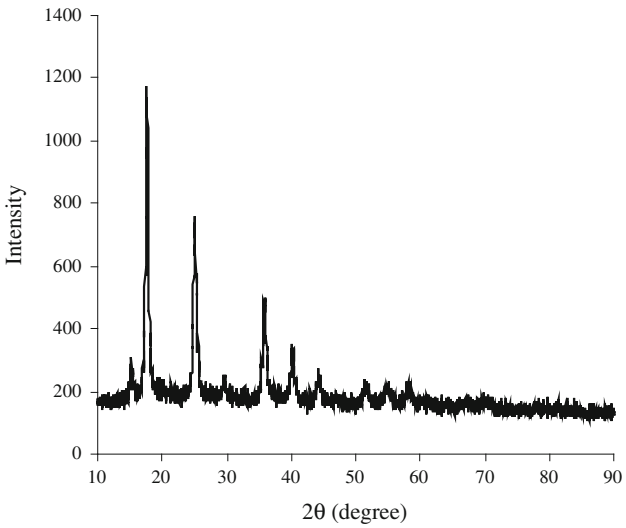

Fig. 1 XRD patterns for the adsorbent

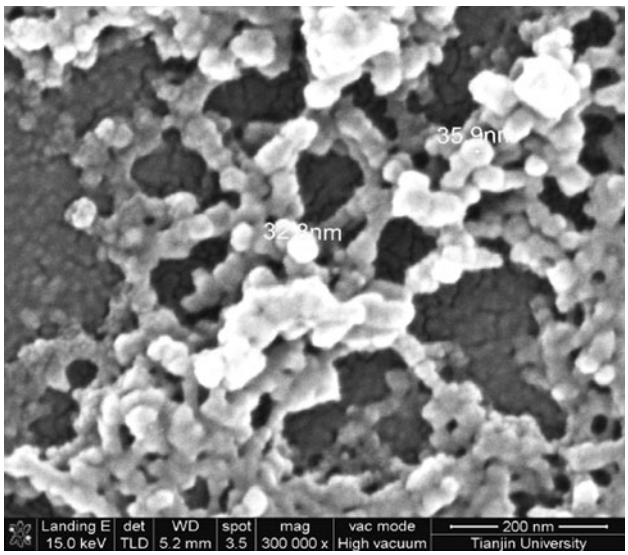

Fig. 2 SEM image of CuFC

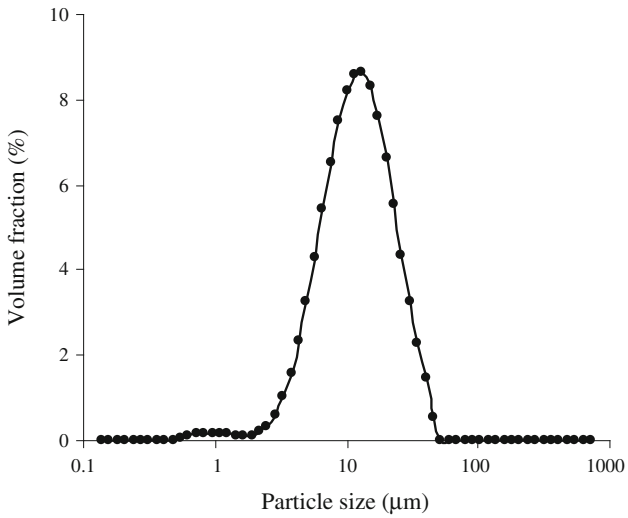

Fig. 3 The particle size distribution of the CuFC suspension

of the microfiltration membranes used to filter the supernatant was 0.22 μm, which was smaller than the particle size of the adsorbent; therefore, the membrane could reject the adsorbent particle completely.

Adsorption kinetics model

The study of adsorption kinetics is desirable because it provides information about the mechanism of adsorption. Adsorption kinetics can be modeled by the intraparticle diffusion model [25], a pseudo-first order model [26] or a pseudo-second order model [27]. The related equations are given as Eq. (4–6), respectively.

$$q_t = k_{id} t^{1/2} + C \tag{4}$$

$$\ln(q_e - q_t) = \ln q_e - k_1 t \tag{5}$$

$$\frac{t}{q_t} = \frac{1}{k_2 q_e^2} + \frac{1}{q_e} t \tag{6}$$

where k_{id} is the initial rate constant of the intraparticle diffusion model (μg/g $\text{min}^{1/2}$); C is the intraparticle diffusion constant (μg/g); k_1 is the rate constant of the pseudo-first order model (1/min); k_2 is the rate constant of the pseudo-second order model (g/μg min). The plots of q_t versus $t^{1/2}$, $\ln(q_e - q_t)$ versus t and t/q_t versus t should be straight lines. The experimental data were fitted with the three models at temperatures of 288, 298 and 308 K, respectively.

Figures 4 and 5 show plots of the linearized form of the intraparticle diffusion model and the pseudo-first order model at different temperatures for the entire adsorption time. However, the experimental data deviated considerably from the theoretical values for both models. It might be that these models were only suited for the initial period of adsorption and could not describe the integrated process of the adsorption [27]. This suggested that the intraparticle diffusion model and the pseudo-first order model were not appropriate for the adsorption of Cs^+ on CuFC.

The pseudo-second order kinetic plot at different temperatures is presented in Fig. 6. It shows that the experimental data fit very well with the calculated values of the pseudo-second order kinetic model for the entire adsorption time at different temperatures. The corresponding parameters could be obtained from the slope and the intercept of the lines; the results are given in Table 1. It can be seen that the rate constant k_2 increased with increasing temperature; the theoretical q_e values were the same as the

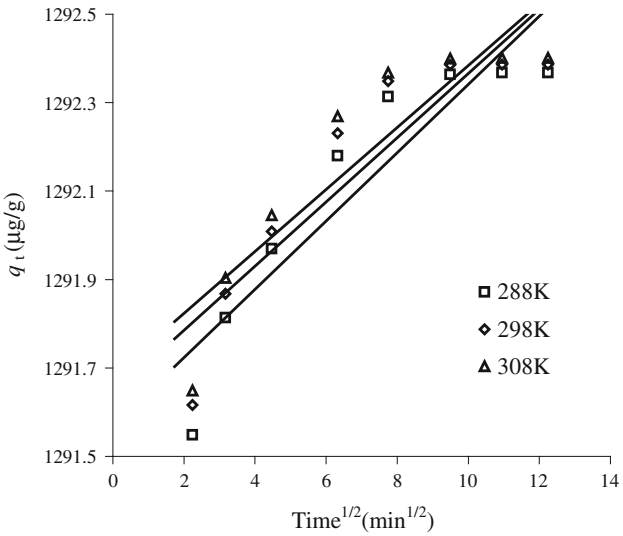

Fig. 4 Intraparticle diffusion kinetics plot at different temperatures

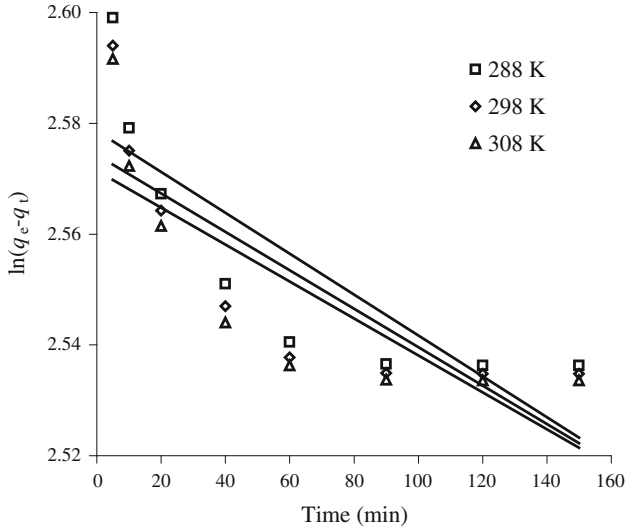

Fig. 5 Pseudo-first order kinetic plot at different temperatures

experimental data, and all of the values for the correlation coefficient R^2 were 1.000 at different temperatures. These results suggested that Cs^+ adsorption on CuFC was best described by a pseudo-second order kinetic model. This model is based on the assumption that the rate determining step may be chemisorption involving valence forces through the sharing or exchange of electrons between the adsorbent and the adsorbate [27, 28].

Adsorption isotherm

The adsorption isotherm parameters actually show the surface properties and affinity of the adsorbent [29]. The Langmuir, Freundlich and Dubinin-Radushkevich (D-R) isotherm models were applied to calculate the adsorption

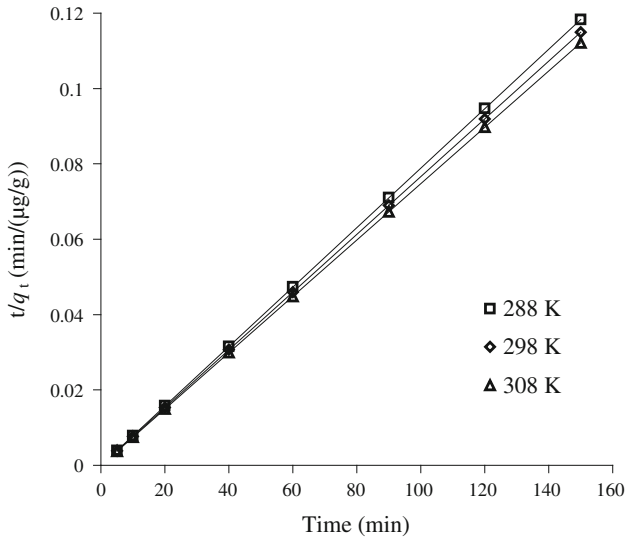

Fig. 6 Pseudo-second order kinetic plot at different temperatures

Table 1 The parameters of the pseudo-second order kinetic model for Cs^+ adsorption on CuFC at different temperatures

Temperature (K)	k_2 (g/μg min)	q_e (μg/g)		R^2
		Calculated	Experimental	
288	0.1492	1,267	1,267	1.000
298	0.1655	1,305	1,305	1.000
308	0.1771	1,337	1,337	1.000

data for Cs^+ on CuFC at temperatures of 288, 298 and 308 K, respectively, in this study.

The Langmuir isotherm model assumes that molecules are adsorbed at a fixed number of well-defined sites, each of which can only hold one molecule and no trans-migration of the adsorbate in the plane of the surface [13]. The form of the Langmuir isotherm is represented by the following equation:

$$q_e = \frac{Q^o b C_e}{1 + bC_e} \tag{7}$$

where Q^0 is the monolayer maximum adsorption capacity (μg/g); b is the Langmuir constant related to the energy of adsorption (L/μg). The linear form of the Langmuir isotherm, shown in Eq. (8), can be obtained by taking the reciprocal of both sides of Eq. (7):

$$\frac{1}{q_e} = \frac{1}{Q^o b}\frac{1}{C_e} + \frac{1}{Q^o} \tag{8}$$

The Freundlich isotherm model is generally regarded as empirical, and it allows for several kinds of adsorption sites on the solid and represents properly the adsorption data at low and intermediate concentrations on heterogeneous surfaces [29]. The model has the following form:

$$\log q_e = \log K_F + \frac{1}{n}\log C_e \tag{9}$$

where K_F ((μg/mg) (L/μg)$^{1/n}$) and $1/n$ are the Freundlich capacity and intensity constants, respectively.

The Dubinin-Raduskevich (D-R) isotherm model is more general than the Langmuir isotherm model because it does not assume a homogeneous surface or constant adsorption potential [28, 30]. The linear form of the D-R equation is

$$\ln q_e = \ln q_{max} - K'\varepsilon^2 \tag{10}$$

where q_e is the Cs^+ concentration in the solid at equilibrium (mol/g); q_{max} is the maximum adsorption capacity (mol/g); K' is the constant related to the mean free energy of the adsorption per mole of the adsorbate (mol^2/kJ^2); ε is the Polanyi potential (kJ/mol), and it is equal to

$$\varepsilon = RT\ln\left(1 + 1/C_{eq}\right) \tag{11}$$

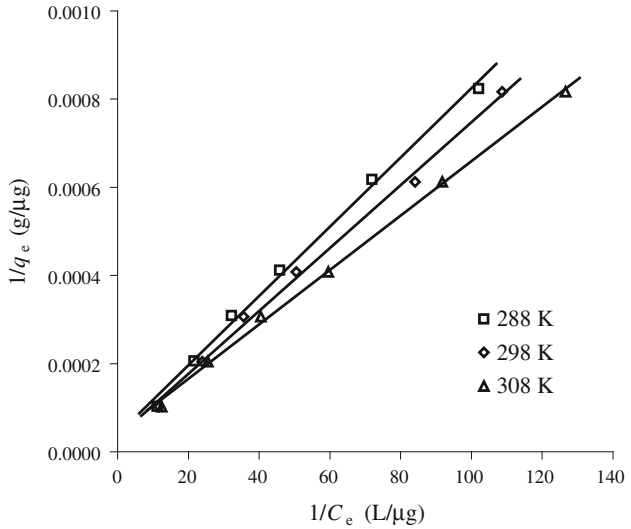

Fig. 7 Linear form of the Langmuir isotherm at different temperatures

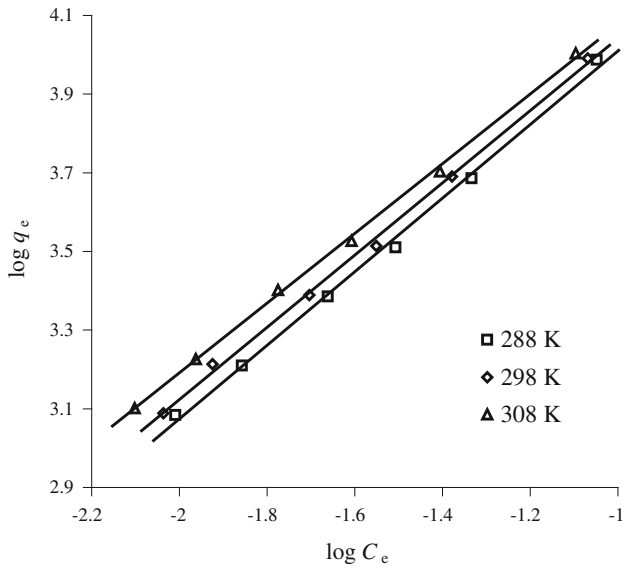

Fig. 8 Linear form of the Freundlich isotherm at different temperatures

where C_{eq} is the Cs^+ concentration in the solution at equilibrium (mol/L); R is the gas constant (8.314×10^{-3} kJ/mol K); and T is the absolute temperature (K).

Linear plots of $1/q_e$ versus $1/C_e$, $\log q_e$ versus $\log C_e$ and $\ln q_e$ versus ε^2 at different temperatures are shown in Figs. 7, 8 and 9. The corresponding parameters calculated from the intercepts and the slopes of the straight lines are given in Table 2.

Figures 7, 8 and 9 show that the experimental data and the calculated values of the Langmuir, Freundlich and D-R models presented a very good linear relationship at all of the temperatures studied. From the obtained high

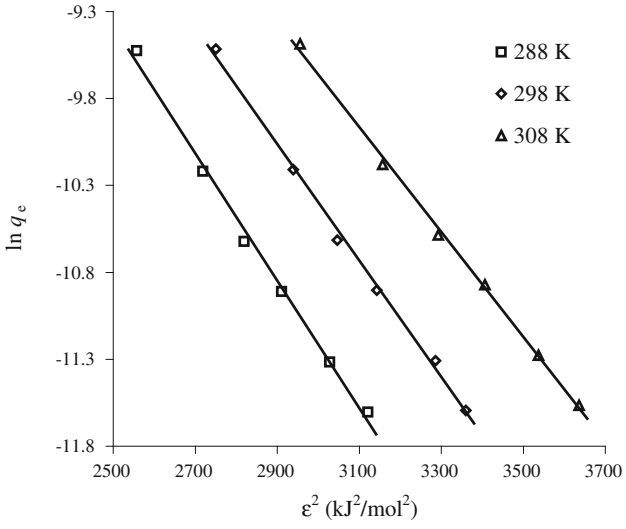

Fig. 9 Linear form of the Dubinin-Radushkevich isotherm at different temperatures

correlation coefficient ($R^2 > 0.99$) values for the Langmuir, Freundlich and D-R isotherm models (Table 2), it appeared that all of these models were very suitable for the adsorption of Cs^+ on CuFC. The applicability of all the studied isotherm models to the Cs^+ adsorption shows that both monolayer adsorption and the heterogeneous energetic distribution of active sites on the sorbent surface are possible [28].

The mean adsorption energy (E), which is defined as the free energy change when one mole of ion is transferred to the surface of the solid from infinity in the solution, is calculated according to the following equation:

$$E = (2K')^{-1/2} \quad (12)$$

The value of E provides valuable information about the adsorption mechanism [31–33]. If the value of E is between 8 and 16 kJ/mol, ion exchange is the main adsorption process in the system. If the value is less than 8 kJ/mol, physisorption is the main adsorption mechanism [31, 34, 35]. Table 2 shows the values of E obtained at different temperatures, the lowest and highest values were 11.62 and 12.91 kJ/mol, respectively, which indicated that ion exchange is the main mechanism involved in the adsorption of Cs^+ on CuFC. This result was similar to the mechanism of cesium removal by $Cu_2^{II}Fe^{II}(CN)_6$ involving ion exchange between one Cu^{2+} in the framework of $Cu_2^{II}Fe^{II}(CN)_6$ and the Cs^+ in the solution as reported by other researchers [17, 19].

Adsorption thermodynamic parameters

To gain insight into the thermodynamic nature of the adsorption process, the adsorption thermodynamic

Table 2 The parameters of the Langmuir, Freundlich and D-R isotherm of Cs^+ on CuFC at different temperatures

T (K)	Langmuir			Freundlich			Dubinin-Radushkevich			
	Q^o (μg/g)	b (L/μg)	R^2	K_F ((μg/g)(L/μg)$^{1/n}$)	$1/n$	R^2	q_{max} (mol/g)	K' (mol^2/kJ^2)	E (kJ/mol)	R^2
288	2.584×10^4	4.924	0.9958	8.790×10^4	0.9347	0.9970	0.7961	0.0037	11.62	0.9951
298	2.933×10^4	4.776	0.9964	9.105×10^4	0.9180	0.9980	0.7071	0.0034	12.13	0.9968
308	2.475×10^4	6.745	0.9984	9.202×10^4	0.8865	0.9988	0.5414	0.0030	12.91	0.9980

parameters, including the changes in the standard Gibbs free energy (ΔG^o), the standard enthalpy (ΔH^o) and the standard entropy ($\Delta S°$), were calculated at a CuFC dose of 80 mg/L and temperatures of 288, 298 and 308 K. The ΔG^o is the fundamental criterion of spontaneity and is given by the following equation [35, 36]:

$$\Delta G^o = -RT \ln K_c \quad (13)$$

where ΔG^o is the change in the standard Gibbs free energy (kJ/mol); K_c is the equilibrium constant, which is independent on the quantity of the adsorbent and the volume of the solution. The value of K_c can be calculated by Eq. (14):

$$K_c = \frac{F_e}{1 - F_e} \quad (14)$$

where F_e is the fractional conversion of the adsorption at equilibrium.

The equilibrium constant (K_c) for the adsorption of Cs^+ ions on CuFC was calculated at different temperatures using Eq. (14). The variation in K_c with temperature, as summarized in Table 3, showed that K_c values increase with an increase in the adsorption temperature, thus implying a strengthening of the adsorbate–adsorbent interactions at higher temperatures [37]. The obtained negative values of the ΔG^o (Table 3) confirmed the feasibility of the process and the spontaneous nature of the adsorption processes. Additionally, the decreasing value of the ΔG^o with increasing temperature indicated that Cs^+ adsorption on the CuFC was more spontaneous at higher temperatures.

The change in the Gibbs free energy can be represented as follows:

$$\Delta G^o = \Delta H^o - T\Delta S^o \quad (15)$$

Table 3 Thermodynamic parameters for Cs^+ adsorption on CuFC

T (K)	K_c	ΔG^o (kJ/mol)	ΔH^o (kJ/mol)	ΔS^o (kJ/mol K)
288	9.913×10^3	−22.03		
298	1.065×10^4	−22.98	9.426	0.1091
308	1.278×10^4	−24.21		

where ΔH^o is the change in the standard enthalpy (kJ/mol); ΔS^o is the change in the standard entropy (kJ/mol K).

The ΔH^o and ΔS^o were calculated from the intercept and slope of the straight line obtained from plotting ΔG^o versus T (Fig. 10), respectively. The values of ΔH^o and ΔS^o are presented in Table 3.

The positive value of ΔH^o revealed that the adsorption of Cs^+ on CuFC was an endothermic process. The positive value of ΔS^o showed an affinity of the CuFC towards Cs^+ ions and an increased randomness at the solid/solution interface with some structural changes in the adsorbate and adsorbent [37, 38].

Effect of pH

The effect of pH on the adsorption of Cs^+ on CuFC is shown in Fig. 11. It can be seen from Fig. 11 that the order of magnitude of the K_d obtained was over 10^6 mL/g when the pH of the solution was between 2.6 and 10.9. This suggests that CuFC could effectively adsorb Cs^+ at a wide pH range [24]. The K_d increased with increasing pH at a pH range of 2.1–9.0. This may be attributed to the fact that both Cs^+ and H^+ ions have the tendency to adsorb on CuFC, and the increasing pH decreases the concentration of H^+ in the solution. Therefore, the active sites on the surface of the CuFC could be occupied by more Cs^+, and the values of K_d would increase [13]. The order of magnitude of K_d decreased below 10^5 mL/g when the pH in the solution was more than 11.9. That may be because the CuFC decomposed into $Cu(OH)_2$ under alkaline conditions [24]. This result was in agreement with a study that showed that all of the ferrocyanide solid was chemically stable over a pH range of approximately 11 maximum to moderately acidic solutions [39].

Effect of K^+ and Na^+

The effect of the K^+ and Na^+ ion concentrations in the solution on the adsorption of Cs^+ to CuFC is shown in Fig. 12. The values of K_d remained constant when the K^+ and Na^+ ion concentrations in the solution were below 20 and 1,000 mg/L, respectively. However, the values of K_d

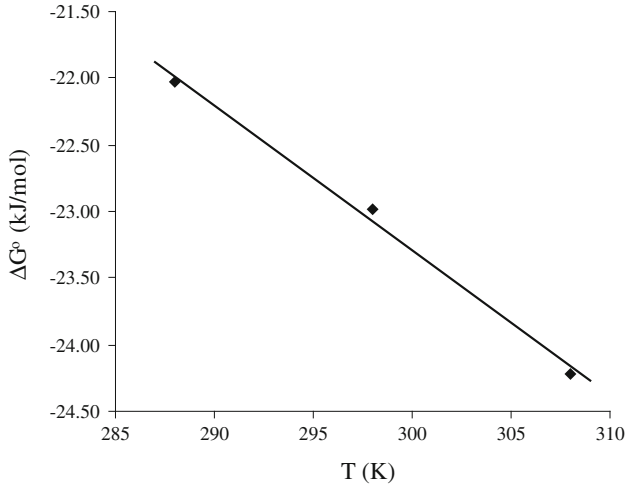

Fig. 10 The relationship between the change in Gibbs free energy and temperature of the adsorption of Cs^+ on CuFC at different temperatures

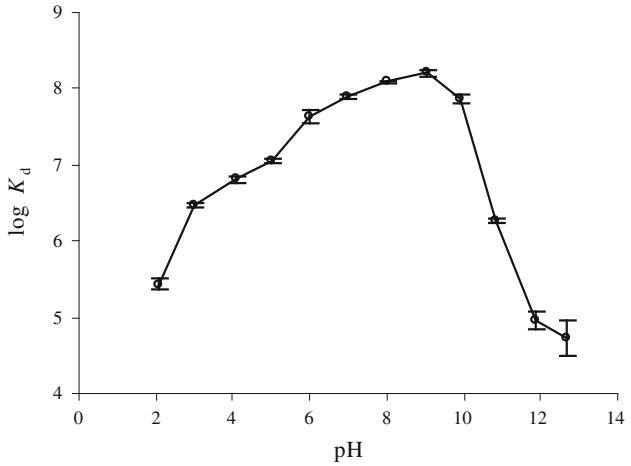

Fig. 11 Effect of pH on the adsorption of Cs^+ on CuFC

decreased drastically when the K^+ and Na^+ ion concentrations in the solution were greater than 40 and 2,000 mg/L, respectively. This result also showed that K^+ had more of an influence on the adsorption of Cs^+ on CuFC than the Na^+ in the solution. Meanwhile, it also confirmed that the affinity of the alkali metal bound to the CuFC in this study increased in the order $Na < K < Cs$. In addition, potassium, sodium and cesium usually exist as valence cations in the solution, and high concentrations of K^+ or Na^+ could produce competitive adsorption with Cs^+, thus making K_d decrease [40].

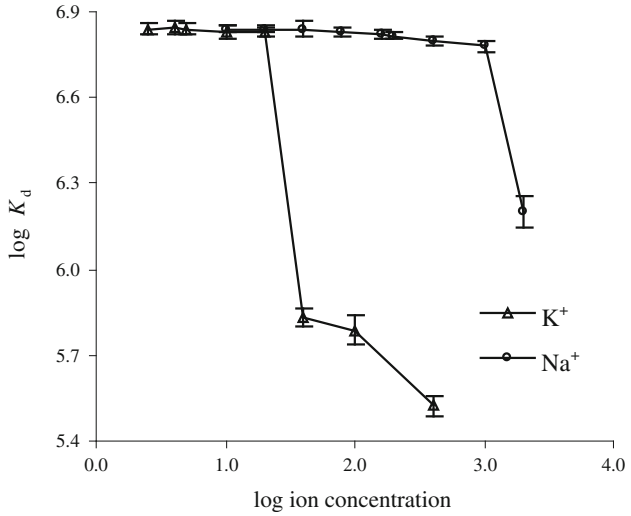

Fig. 12 Effect of K^+ and Na^+ concentrations on the adsorption of Cs^+ on CuFC

Conclusion

CuFC with clear geometric shapes was prepared from sodium ferrocyanide and copper nitrate. Cs^+ adsorption on CuFC was best described by a pseudo-second order kinetic model. The adsorption isotherm could be described by the Langmuir, Freundlich or D-R model, and ion exchange was the main mechanism during the adsorption process. The adsorption of Cs^+ on CuFC was an endothermic and spontaneous reaction and was more spontaneous at higher temperatures. The CuFC had an excellent adsorption effect on Cs^+ at a pH range of 2.6–10.9, and the order of magnitude of the K_d obtained was more than 10^6 mL/g. The existence of K^+ and Na^+ did not affect the adsorption of Cs^+ on CuFC when the concentrations of K^+ and Na^+ in the solution were below 20 and 1,000 mg/L, respectively.

Acknowledgements The authors are grateful for financial support from the National Nature Science Foundation of China (51178301).

References

1. Manolopoulou M, Vagena E, Stoulos S, Ioannidou A, Papastefanou C (2011) Radioiodine and radiocesium in Thessaloniki, Northern Greece due to the Fukushima nuclear accident. J Environ Radioact 102:796–797
2. Valsala TP, Roy SC, Shah JG, Gabriel J, Raj K, Venugopal V (2009) Removal of radioactive caesium from low level radioactive waste (LLW) streams using cobalt ferrocyanide impregnated organic anion exchanger. J Hazard Mater 166:1148–1153
3. Murali MS, Raut DR, Prabhu DR, Mohapatra PK, Tomar BS, Manchanda VK (2012) Removal of Cs from simulated high-level waste solutions by extraction using chlorinated cobaltdicarbollide

in a mixture of nitrobenzene and xylene. J Radioanal Nucl Chem 291:611–616
4. Peterson RA, Burgess JO, Walker DD, Hobbs DT, Serkiz SM, Barnes MJ, Jurgensen AR (2001) Decontamination of high-level waste using a continuous precipitation process. Sep Sci Technol 36:1307–1321
5. Lin Y, Fryxell GE, Wu H, Engelhard M (2001) Selective sorption of cesium using self-assembled monolayers on mesoporous supports. Environ Sci Technol 35:3962–3966
6. Raut DR, Mohapatra PK, Ansari SA, Manchanda VK (2008) Evaluation of a calix[4]-bis-crown-6 ionophore-based supported liquid membrane system for selective ^{137}Cs transport from acidic solutions. J Membr Sci 310:229–236
7. Mohapatra PK, Bhattacharyya A, Manchanda VK (2010) Selective separation of radio-cesium from acidic solutions using supported liquid membrane containing chlorinated cobalt dicarbollide (CCD) in phenyltrifluoromethyl sulphone (PTMS). J Hazard Mater 181:679–685
8. Anthony RG, Dosch RG, Gu D, Philip CV (1994) Use of silicotitanates for removing cesium and strontium from defense waste. Ind Eng Chem Res 33:2702–2705
9. Solbra S, Allison N, Waite S, Mikhalovsky SV, Bortun AI, Bortun LN, Clearfield A (2001) Cesium and strontium ion exchange on the framework titanium silicate $M_2Ti_2O_3$-$SiO_4{\cdot}nH_2O$(M = H, Na). Environ Sci Technol 35:626–629
10. Borai EH, Harjula R, Malinen L, Paajanen A (2009) Efficient removal of cesium from low-level radioactive liquid waste using natural and impregnated zeolite minerals. J Hazard Mater 172: 416–422
11. Shady SA (2009) Selectivity of cesium from fission radionuclides using resorcinol-formaldehyde and zirconyl-molybdopyrophosphate as ion-exchangers. J Hazard Mater 167:947–952
12. Park Y, Lee Y-C, Shin WS, Choi S-J (2010) Removal of cobalt, strontium and cesium from radioactive laundry wastewater by ammonium molybdophosphate-polyacrylonitrile (AMP-PAN). Chem Eng J 162:685–695
13. Nilchi A, Saberi R, Moradi M, Azizpour H, Zarghami R (2011) Adsorption of cesium on copper hexacyanoferrate - PAN composite ion exchanger from aqueous solution. Chem Eng J 172:572–580
14. Avramenko V, Bratskaya S, Zheleznov V, Sheveleva I, Voitenko O, Sergienko V (2011) Colloid stable sorbents for cesium removal: preparation and application of latex particles functionalized with transition metals ferrocyanides. J Hazard Mater 186: 1343–1350
15. Sangvanich T, Sukwarotwat V, Wiacek RJ, Grudzien RM, Fryxell GE, Addleman RS, Timchalk C, Yantasee W (2010) Selective capture of cesium and thallium from natural waters and simulated wastes with copper ferrocyanide functionalized mesoporous silica. J Hazard Mater 182:225–231
16. Loos-Neskovic C, Ayrault S, Badillo V, Jimenez B, Garnier E, Fedoroff M, Jones DJ, Merinov B (2004) Structure of copper-potassium hexacyanoferrate (II) and sorption mechanisms of cesium. J Solid State Chem 177:1817–1882
17. Sinha PK, Amalraj RV, Krishnasamy V (1993) Flocculation studies on freshly precipitated copper ferrocyanide for the removal of caesium from radioactive liquid waste. Waste Manage 13:341–350
18. Ayrault S, Loos-Neskovic C, Fedoroff M, Gamier E, Jones DJ (1995) Compositions and structures of copper hexacyanoferrates(II) and (III): experimental results. Talanta 42:1581–1593
19. Ayrault S, Jimenez B, Garnier E, Fedoroff M, Jones DJ, Loos-Neskovic C (1998) Sorption mechanisms of cesium on Cu_2^{II}-$Fe^{II}(CN)_6$ and $Cu_3^{II}[Fe^{III}(CN)_6]_2$ hexacyanoferrates and their relation to the crystalline structure. J Solid State Chem 141: 475–485
20. Lee EFT, Streat M (1983) Sorption of caesium by complex hexacyanoferrates V. A comparison of some cyanoferrates. J Chem Technol Biotechnol 33A:333–338
21. Lee EFT, Streat M (1983) Sorption of caesium by complex hexacyanoferrates III. A study of the sorption properties of potassium copper ferrocyanide. J Chem Technol Biotechnol 33A:80–86
22. Zhang C-P, Gu P, Zhao J, Zhang D, Deng Y (2009) Research on the treatment of liquid waste containing cesium by an adsorption-microfiltration process with potassium zinc hexacyanoferrate. J Hazard Mater 167:1057–1062
23. Vrtoch L, Pipíška M, Horník M, Augustín J, Lesný J (2011) Sorption of cesium from water solutions on potassium nickel hexacyanoferrate-modified *Agaricus bisporus* mushroom biomass. J Radioanal Nucl Chem 287:853–862
24. Haas PA (1993) A review of information on ferrocyanide solids for removal of cesium from solutions. Sep Sci Technol 28: 2479–2506
25. Weber WJ, Morris JC (1963) Kinetics of adsorption on carbon from solution. J Sanit Eng Div ASCE 89:31–39
26. Ho YS, McKay G (1999) The sorption of lead(II) ions on peat. Water Res 33:578–584
27. Ho YS, McKay G (1999) Pseudo-second order model for sorption processes. Process Biochem 34:451–465
28. Namasivayam C, Sureshkumar MV (2008) Removal of chromium(VI) from water and wastewater using surfactant modified coconut coir pith as a biosorbent. Bioresour Technol 99:2218–2225
29. Saberi R, Nilchi A, Garmarodi SR, Zarghami R (2010) Adsorption characteristic of ^{137}Cs from aqueous solution using PAN-based sodium titanosilicate composite. J Radioanal Nucl Chem 284:461–469
30. Metwally E, El-Zakla T, Ayoub RR (2008) Thermodynamics study for the sorption of ^{134}Cs and ^{60}Co radionuclides from aqueous solutions. J Nucl Radiochem Sci 9:1–6
31. Atun G, Kilislioglu A (2003) Adsorption behavior of cesium on montmorillonite-type clay in the presence of potassium ions. J Radioanal Nucl Chem 258:605–611
32. Crittenden JC, Sanongraj S, Bulloch JL, Hand DW, Rogers TN, Speth TF, Ulmer M (1999) Correlation of aqueous-phase adsorption isotherms. Environ Sci Technol 33:2926–2933
33. Stoeckli F, López-Ramón MV, Moreno-Castilla C (2001) Adsorption of phenolic compounds from aqueous solutions, by activated carbons, described by the Dubinin-Astakhov equation. Langmuir 17:3301–3306
34. Helfferich F (1962) Ion exchange. Mc Graw Hill, New York
35. Cortés-Martínez R, Olguín MT, Solache-Ríos M (2010) Cesium sorption by clinoptilolite-rich tuffs in batch and fixed-bed systems. Desalination 258:164–170
36. Kashi Banerjee GLA, Prevostc Michele et al (2008) Kinetic and thermodynamic aspects of adsorption of arsenic onto granular ferric hydroxide (GFH). Water Res 42:3371–3378
37. El-Naggar IM, Zakaria ES, Ali IM, Khalil M, El-Shahat MF (2012) Kinetic modeling analysis for the removal of cesium ions from aqueous solutions using polyaniline titanotungstate. Arabian Journal of Chemistry 5:109–119
38. Hassan HS, Attallah MF, Yakout SM (2010) Sorption characteristics of an economical sorbent material used for removal radioisotopes of cesium and europium. J Radioanal Nucl Chem 286:17–26
39. Campbell DO, Lee DD, Dillow TA (1991) Development studies for the treatment of ORNL low-level liquid waste. ORNL/TM-11798. Oak Ridge National Laboratory, Oak Ridge
40. Yavari R, Huang YD, Ahmadi SJ, Bagheri G (2010) Uptake behavior of titanium molybdophosphate for cesium and strontium. J Radioanal Nucl Chem 286:223–229